Ship-in-a-bottle CMPO in MIL-101(Cr) for selective uranium recovery from aqueous streams through adsorption

Title: Ship-in-a-bottle CMPO in MIL-101(Cr) for selective uranium recovery from aqueous streams through adsorption

Authors: Jeroen De Decker, Karel Folens, Jeriffa De Clercq, Maria Meledina, Gustaaf Van Tendeloo, Gijs Du Laing, Pascal Van Der Voort

PII: S0304-3894(17)30271-6
DOI: http://dx.doi.org/doi:10.1016/j.jhazmat.2017.04.029
Reference: HAZMAT 18512

To appear in: *Journal of Hazardous Materials*

Received date: 10-3-2017
Revised date: 6-4-2017
Accepted date: 8-4-2017

Please cite this article as: Jeroen De Decker, Karel Folens, Jeriffa De Clercq, Maria Meledina, Gustaaf Van Tendeloo, Gijs Du Laing, Pascal Van Der Voort, Ship-in-a-bottle CMPO in MIL-101(Cr) for selective uranium recovery from aqueous streams through adsorption, Journal of Hazardous Materialshttp://dx.doi.org/10.1016/j.jhazmat.2017.04.029

Ship-in-a-bottle CMPO in MIL-101(Cr) for selective uranium recovery from aqueous streams through adsorption

De Decker Jeroen[1], Folens Karel[2], De Clercq Jeriffa[3], Maria Meledina[4], Gustaaf Van Tendeloo[4], Du Laing Gijs[2], Van Der Voort Pascal[1*]

[1] Department of Inorganic and Physical Chemistry, Center for Ordered Materials, Organometallics, and Catalysis (COMOC), Ghent University, Krijgslaan 281-S3, 9000 Ghent, Belgium.

[2] Laboratory of Analytical Chemistry and Applied Ecochemistry, Ghent University, Coupure Links 653, 9000 Ghent, Belgium.

[3] Department of Materials, Textiles, and Chemical Engineering. Industrial Catalysis and Adsorption Technology (INCAT). Ghent University, Valentin, Vaerwyckweg 1, 9000 Ghent, Belgium.

[4] EMAT, University of Antwerp, Groenenborgerlaan 171, 2020 Antwerp, Belgium.

*Corresponding author: Pascal van der Voort (pascal.vandervoort@ugent.be)

Highlights

- Highly stable metal-organic framework, MIL-101(Cr), for uses in aqueous, acidic adsorption
- Uranium recovery from low concentration acidic solutions
- One-step ship-around-the-bottle synthetic approach to incorporate CMPO in MIL-101(Cr)
- Highly selective U(VI) adsorbent in competition with a high variety of metals, incl. rare earths and transition metals
- Regenerable and reusable adsorbent via 0.1 M nitric acid stripping

Abstract

Mesoporous MIL-101(Cr) is used as host for a ship-in-a-bottle type adsorbent for selective U(VI) recovery from aqueous environments. The acid-resistant cage-type MOF is built in-situ around N,N-Diisobutyl-2-(octylphenylphosphoryl)acetamide (CMPO), a sterically demanding ligand with high U(VI) affinity. This one-step procedure yields an adsorbent which is an ideal compromise between homogeneous and heterogeneous systems, where the ligand can act freely within the pores of MIL-101, without leaching, while the adsorbent is easy separable and reusable. The adsorbent was characterized by XRD, FTIR spectroscopy, nitrogen adsorption, XRF, ADF-STEM and EDX, to confirm and quantify the successful encapsulation of the CMPO in MIL-101, and the preservation of the host. Adsorption experiments with a central focus on U(VI) recovery were performed. Very high selectivity for U(VI) was observed, while competitive metal adsorption (rare earths, transition metals…) was almost negligible. The adsorption capacity was calculated at 5.32 mg U/g (pH 3) and 27.99 mg U/g (pH 4), by fitting equilibrium data to the Langmuir model. Adsorption kinetics correlated to the pseudo-second-order model, where more than 95 % of maximum uptake is achieved within 375 minutes. The adsorbed U(VI) is easily recovered by desorption in 0.1 M HNO_3. Three adsorption/desorption cycles were performed.

Keywords: *Metal-Organic Frameworks • Adsorption • Uranium • Environmental Chemistry*

1. Introduction

According to the International Energy Outlook Reference case (IEO2016), the total world energy consumption is projected to increase by 48% between 2012 and 2040. With renewables as the number one fastest-growing energy source, nuclear power occupies second place with a projected annual consumption increase of 2.3%. Even though the consumption of non-fossil fuels is expected to grow faster than the consumption of fossil fuels, the latter will still account for 78% of the energy use in 2040[1]. Meanwhile, the world has to deal with environmental threats caused by anthropogenic polluting emissions. Nuclear energy provides a significant part of the energy (electricity) demand, combined with a reduction in polluting emissions. Uranium fuel will remain to play a key role in energy production, with the rise of next generation light water reactors, which are expected to dominate the world market in the first half of the 21st century[2]. However, as the demand for nuclear fuel rises, equal effort should be made to close the nuclear fuel cycles (recyclability) or to optimize current processes with clear and effective waste management strategies. At the 2012 level of uranium requirements, currently identified resources (2013) are sufficient for over 120 years of supply for the global nuclear power fleet (5.9 million tons in the <USD 130/kg U category)[3]. This calls for uranium extraction and recovery from sources other than the conventional orebodies. Unconventional resources (where uranium is present as a by-product or as traces) include phosphate rocks, non-ferrous ores, carbonatite, black shale, lignite, and seawater[3-5]. With the proper (economically feasible) techniques at hand, these secondary resources could become viable orebodies.

For example, uranium occurs in all types of phosphate rocks with varying concentrations[6]. These rocks are usually leached with acids, as part of the production process of fertilizers, which eventually leads to uranium containing aqueous solutions that constitute as a secondary uranium source[7-9]. The uranium content of both the phosphate rocks, as well as the obtained leachates, lies in the ppm range[5, 9]. In addition to uranium, many other ppm-level impurities, such as Pb, Ni, Cu and Mn may be present[5]. Therefore, selective uranium recovery is necessary and currently, solvent extraction processes and precipitations techniques are typically applied (industrially) to achieve these kinds of selective separations[8, 9]. Despite their effectiveness, however, these conventional techniques usually suffer from economical and/or environmental limitations, due to the labor-intensiveness and high usage of chemicals that are inherent to the respective techniques[9-11].

In addition to being a key raw material for nuclear energy, uranium also causes a long-term potential environmental hazard because of its long half-life and high radio-toxicity[12-14]. In the case of rare earth mining, uranium is often present in the minerals via lattice substitution, resulting in radiation issues in rare earth processing[15]. Also in ion-adsorption clays, mainly found in China, there is a considerable amount of uranium present (ppm range). These clays are rich in yttrium and heavy rare earths (HREE), and are the main source for the world's HREE production. No measures are taken in controlling the uranium radiation due to its low concentrations in the clays[15]. An appropriate method to selectively separate the uranium from these valuable rare earths is therefore desired.

These are but a few examples of uranium-containing sources that would benefit from recovery techniques optimized for low concentrated, aqueous streams. Selective adsorption is an ideal technique to recover specific species from such dilute solutions. Adsorbents are readily tunable to preference and the added value of easy separation and reuse makes them perfect candidates for this field of metal recovery. Over the past decades, various materials have been successfully applied as metal targeting adsorbents, both pristinely and functionalized, e.g., activated carbon[16, 17], lignin[18, 19], carbon nanotubes[20], zeolites[21], clays[22], porous silicas[23, 24], metal oxides[25]... Novel adsorbents are of high interest, not only to extract uranium from secondary orebodies for nuclear fuel production, but also for the removal of these toxic radionuclides from waste streams and acid mine drainage[4, 11, 26-28]. Metal–organic frameworks (MOFs) could play a big role in the development of new water-applicable adsorbents. This class of porous coordination polymers consists of highly uniform networks of inorganic metal centers (ions or clusters), bridged with polytopic organic ligands as linkers. By varying these metal centers and/or linkers, a vast amount of different MOFs can be synthesized, each with its specific physicochemical properties, including water-stable MOFs [29]. Due to this remarkable versatility, MOFs have already been applied in a broad range of research fields, such as gas storage and separation[30-33], catalysis[34, 35], separation of chemicals[36, 37], drug delivery[38, 39], magnetism[40], luminescence[41]… When dealing with aqueous metal adsorption, the conditions are often very demanding and additional stability in acidic and/or alkaline media is required[29]. Several types of MOFs meet these criteria, such as MOF-76, (NH_2-)UiO-66, NH_2-MIL-53, MIL-101(Cr)…[42, 43], which often show remarkable stability even during long-term exposure to these conditions. Recently, it was reported that MOFs could be applied as potential uranium adsorbents, e.g., Zn-MOF-74, Ln-MOF-76, UiO-68, and MIL-101(Cr) have been functionalized (Zn-MOF-74, UiO-68, MIL-101) or used pristinely (Ln-MOF-76) to recover uranium from aqueous environment[42, 44-46].

In this work, we have selected MIL-101(Cr) as a highly stable, mesoporous host for the embedment of N,N-Diisobutyl-2-(octylphenylphosphoryl)acetamide (CMPO), a sterically demanding, commercially available ligand known for its high affinity with U(VI). The mesoporous zeotypic MIL-101 cages with diameters of ca. 29 and 34 Å are ideal to enclose the CMPO, while the microporous cage-apertures (12 – 16 Å) are small enough to contain it, yet large enough to facilitate the transportation of metal cations through the pore network. CMPO is often used as a highly efficient (co-)extractant for actinides and lanthanides in solvent extraction processes, such as the trans-uranium extraction process (TRUEX)[47, 48]. The CMPO ligand was embedded in the MIL-101 host, through the bottle-around-the-ship approach, in which the host is formed in-situ around the CMPO. This approach is cost- and time effective, when compared to conventional adsorbent synthesis where the host is pre-synthesized, followed by a single or multistep post-functionalization. The obtained materials were properly characterized by X-ray diffraction (XRD), nitrogen adsorption, FT-IR spectrometry, X-ray fluorescence spectrometry and a combination of ADF-STEM (annular dark field scanning transmission electron microscopy) and EDX (energy dispersive X-ray) spectroscopy. An extensive U(VI) centered adsorption study was performed, including equilibrium experiments, kinetics, selectivity, pH-influence, regeneration, and reuse, to investigate the viability of this novel material as a selective, reusable uranium adsorbent.

2. Experimental

2.1 Chemicals and Reagents

Single-element standard solutions (1000 mg/L) for ICP-OES analysis were obtained from Chem-Lab, Belgium. Uranium(VI) standard solution (10000 mg/L in 1% HNO_3) was obtained from J.T.Baker, The Netherlands, and was used for adsorption experiments. N,N-Diisobutyl-2-octylphenylphosphoryl) acetamide (CMPO) was obtained from Carbosynth Ltd, United Kingdom. $CdSO_4 \cdot 2\ H_2O$ and $Al_2(SO_4)_3 \cdot 18\ H_2O$ were obtained from Chem-Lab, Belgium, and $CoSO_4 \cdot 7\ H_2O$, $CuSO_4 \cdot 5\ H_2O$, $MnSO_4 \cdot H_2O$, and $ZnSO_4 \cdot 7\ H_2O$ from Merck, United States. $NiSO_4 \cdot 6\ H_2O$ and $PbSO_4$ were obtained from UCB, Belgium. All remaining chemicals were obtained from Sigma Aldrich, Belgium. All chemicals were used as received, without further purification.

2.2 Synthesis of Ship-in-a-Bottle CMPO in MIL-101(Cr)

N,N-Diisobutyl-2-(octylphenylphosphoryl)acetamide (CMPO, MW: 407.6 g/mol, 0.16 mmol) was ground into a fine powder with mortar and pestle and added to a Teflon-lined autoclave containing 20 mL of deionized water. Terephthalic acid (4 mmol) and $Cr(NO_3)_3 \cdot 9H_2O$ (4 mmol) were added to this suspension (according to [49]). The autoclave was heated to 210 °C for 8 hours (2 hours warm-up) under autogenous pressure. After cooling to room temperature, the product was filtered off and washed thoroughly with 1 M HCl solution (at RT) and dimethylformamide (DMF) at 60°C respectively (overnight), in order to purify the material from leftover and/or clogged reagents. The material was once again filtered off and rinsed with acetone, followed by vacuum drying at 120 °C for 24 hours.

2.3 Characterization techniques

Different characterization techniques were applied to map the materials' morphology, surface chemistry and composition. Nitrogen sorption experiments were conducted at 77 K using a Belsorp-mini II gas analyzer. Samples were vacuum dried at 120 °C before measurements. Specific surface areas were calculated using the Langmuir and BET method. Pore volumes were estimated at *p/p0* = 0.90. FTIR (DRIFTS) spectra were recorded on a Nicolet 6700 FTIR spectrometer (Thermo-Scientific) equipped with MCT detector (Analyses performed at 120 °C under vacuum). X-ray fluorescence (XRF) spectroscopy was used to quantify the phosphorous content of the material. The XRF measurements were performed using an energy-dispersive Rigaku NexCG spectrometer. X-ray diffraction analyses (powder) were performed using an ARL X'tra diffractometer (Thermo-Scientific). ADF-STEM and EDX spectroscopy analyses were performed, using a FEI Tecnai Osiris electron microscope operated at 200 kV, equipped with a ChemiSTEM system, to analyze the dispersion of phosphorous throughout the chromium-rich MIL-101(Cr) environment.

2.4 Stability

The stability of the adsorbent was verified by exposure to pH 0 (either 1 M HCl or 1 M HNO_3). 100 mg of adsorbent was magnetically stirred in 50 mL of the respective acid solution for 48 hours. Afterwards, the solids were filtered off, rinsed with distilled water and acetone, followed by vacuum drying at 120 °C. XRD and XRF solid analyses were used to verify the material stability and leaching behavior.

2.5 Adsorption Experiments

The adsorbent was subjected to a series of adsorption experiments, including equilibrium, selectivity, kinetics, pH-dependency, regeneration and reuse experiments. These were carried out in batch setup at room temperature (25 °C). The U(VI) equilibrium experiment was performed with varying initial concentrations (from a 1000 mg/L U(VI) solution, 2% HNO_3). The pH of the initial solutions was set to either 3.0 ± 0.1 or 4.0 ± 0.1 by adding aqueous NaOH solution (0.1 M), followed by short sonication. These two pH levels were chosen since uranium speciation is very pH dependent in this pH-range. The tests were performed in cylindrical plastic tubes, using 10 mg of adsorbent per 10 mL of solution (L/S: 1000 mL/g). The tubes were shaken for 24 hours to ensure equilibrium, using a GFL 3015 orbital shaking device at 200 rpm. Each test was performed in duplicate and the average values are reported. After filtration, using 0.45 µm PET syringe filters, the filtrates (and initial solutions) were analyzed with ICP–OES (Vista MPX, Varian). All solutions were acidified with HNO_3 prior to ICP-OES analysis.
The equilibrium metal adsorption capacity q_e (mg/g) is calculated using the following equation:

$$q_e = \frac{C_0 - C_e}{m}.V$$

where C_0 and C_e are the initial and equilibrium metal concentrations (mg/L) in the solution respectively, V is the solution volume (L) and m equals the adsorbent mass (g).
The experimental data was fitted to the Langmuir and Freundlich model, which are given respectively by the following equations:

$$q_e = \frac{q_{max}.K_L.C_e}{1 + K_L.C_e}$$

$$q_e = K_F.C_e^{1/n}$$

where K_L (L/mg) and K_F (mg/g.(mg/L)$^{1/n}$) are the respective Langmuir and Freundlich constants, q_{max} is the maximum adsorption capacity (mg/g), and n is a constant related to surface heterogeneity.
Selectivity experiments were conducted on a multi-element solution containing Eu(III), Gd(III), Nd(III), Y(III), U(VI), Al(III), Cd(II), Co(II), Cu(II), Mn(II), Ni(II), Pb(II), and Zn(II). The concentration of each metal was ~1 mg/L. Both the adsorbent as well as the pristine MIL-101 were tested in this experiment. The conditions were kept identical to the equilibrium study (L/S: 1000 mL/g and pH 4.0) and samples were filtered and analyzed in the same manner. Each test was performed in triplicate and the average values are reported.
The affinity of the adsorbent for a specific metal is expressed by the distribution coefficient K_d (mL/g), calculated by the following equation:

$$K_d = \frac{C_0 - C_e}{C_e}.\frac{V}{m}$$

To account for analysis inaccuracies, K_d values between -30 and +30 are reported as K_d = 0 mL/g. The original data, including standard deviations are shown in the Supporting Information Fig. S.1.
Kinetic experiments were performed with an initial U(VI) concentration of 30 mg/L (L/S: 1000 mL/g) at pH 3.0. Seven different contact times were considered (5 min, 30 min, 60 min, 120 min, 360 min, 1320 min, and 1440 min). Each test was performed in duplicate and the average values are reported. The experimental data was fitted to both pseudo-first and pseudo–second-order kinetic models, which are given respectively by the following equations (non-linear form):

$$q_t = q_e(1 - e^{-k_1.t})$$

$$q_t = \frac{q_e^2.k_2.t}{1 + k_2 q_e t}$$

where q_t is the amount of adsorbed metal at time t (mg/g), k_1 and k_2 are the respective rate constants of the Lagergren pseudo-first-order model (L/min) and the pseudo-second-order model (g/mg/min).
pH-dependency experiments were performed, in order to get information about: (1) the practical operating pH-range of the adsorbent, (2) the pH level at which the MOF matrix no longer interacts with the adsorbate, (3) the pH level at which regeneration experiments could be performed. The influence of pH on the adsorption was investigated by performing experiments at three different pH levels: 0.5, 3.0, and 6.0, with an initial U(VI) solution of 30 mg/L adjusted with either aq. NaOH (0.1 M) or aq. HNO_3 (0.1 M) to the desired pH level, followed by short sonication. The adsorption experiment was performed analogously to the equilibrium experiments.
Regeneration and reusability experiments were performed by initially saturating the adsorbent with a 100 ppm U(VI) solution at pH 4 (setup similarly to the equilibrium experiments). Afterwards, the solids were filtered off from the suspension and dried under vacuum, whilst the filtrate was analyzed for its uranium concentration. Regeneration was then performed using 0.1 M HNO_3, by shaking at 200 rpm for 24 hours at 25 °C (L/S: 1000 mL/g). The solids were filtered off and dried once again, and the filtrate was analyzed for its uranium content. This comprises one cycle. A total of three cycles were performed.

3 Results and discussion

3.1 Ship-in-a-bottle adsorbent

The CMPO-containing MIL-101 was synthesized through a so-called “bottle-around-the-ship” approach, in which the adsorbent matrix is formed around a molecule of interest. Ideally, this molecule is then trapped in the system, but can still act freely and unhindered within the pores of the host, hence the name of this approach. A ship-in-a-bottle system is a perfect compromise between homogeneous and heterogeneous analogues. The effectiveness of a free homogeneous ligand or other moiety (catalytic complex, biomolecule…) is combined with the advantages of heterogeneous systems (easy separation and reuse). The way several frameworks of MOFs are built up makes them

very interesting for this kind of systems, and already several reports have been published where MOFs are used as matrices for ship-in-a-bottle catalytic systems[50-56]. To our knowledge, MOFs have not yet been applied as ship-in-a-bottle matrix for adsorbents. In this work, MIL-101(Cr) was selected as matrix, owing to its unique characteristics. This particular MOF is both mesoporous and a cage-type MOF (as mentioned above), and is therefore suitable to encapsulate rather bulky molecules (chelating ligands), which are often used as selective complexants. The cage structure itself is made up of microporous windows (12 – 16 Å), which can prevent such bulky moieties from leaving the cages (Fig. 1). In addition, MIL-101(Cr) is one of the few mesoporous MOFs possessing an excellent stability in both acidic and alkaline aqueous environments (short- and long term)[43, 57, 58]. All of these qualities make the MIL-101(Cr) a perfect candidate for uses in aqueous adsorption environments and as a host for the "bottle-around-the-ship" approach.

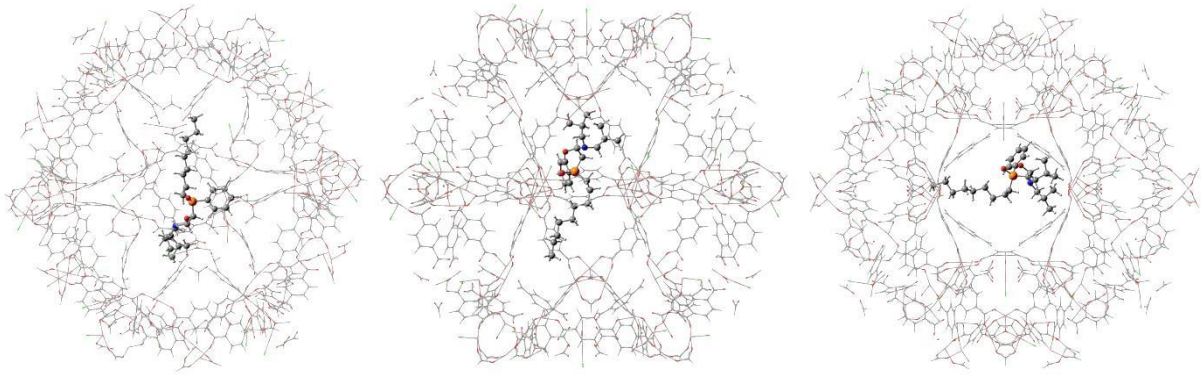

Fig. 1. Visualization of a CMPO molecule trapped in an individual MIL-101(Cr) cage. Three different angles of the cage are represented. The CMPO ligand is visualized in the ball-stick manner, whereas the MIL-101 cage is represented as a wireframe, for clarity reasons. (High-resolution images are provided in the supporting information, Fig. S.2)

3.2 Material characterization

Fig. 2 shows the DRIFTS spectra of the pristine MIL-101(Cr) and the ship-in-a-bottle CMPO in MIL-101, hereafter called MIL-101-Ship. By comparing both spectra to the included pure CMPO spectrum, the presence of CMPO in the structure can be successfully confirmed. A clear indication of aliphatic and aromatic C-H stretches in the MIL-101-Ship spectrum is visible around 2850 – 3000 cm^{-1} and 3010 – 3050 cm^{-1} respectively. Phosphine oxide (P=O) stretching vibrations are observed around 1100 cm^{-1} and an additional aromatic C-H out-of-plane bending vibration is visible as well around 690 cm^{-1}. Other characteristic vibrations of the CMPO are not clearly discernible due to either the overlap with vibrations inherent to MIL-101, or because of the limited ligand loading in the material. Fig. 3 shows the N_2-sorption isotherms and XRD diffractograms for MIL-101 and MIL-101-Ship. In both of the nitrogen adsorption isotherms, the characteristic MIL-101 isotherm shape can be recognized, which indirectly confirms that the addition of CMPO to the synthetic mixture did not prevent the hydrothermal formation of MIL-101. This is further confirmed by XRD where the MIL-101 crystallography is clearly observed in both patterns. Table 1 shows the specific surface areas and pore volumes, as well as phosphorous content (wt. %) as detected by XRF. The calculated CMPO loading (mmol/g) is added as well.

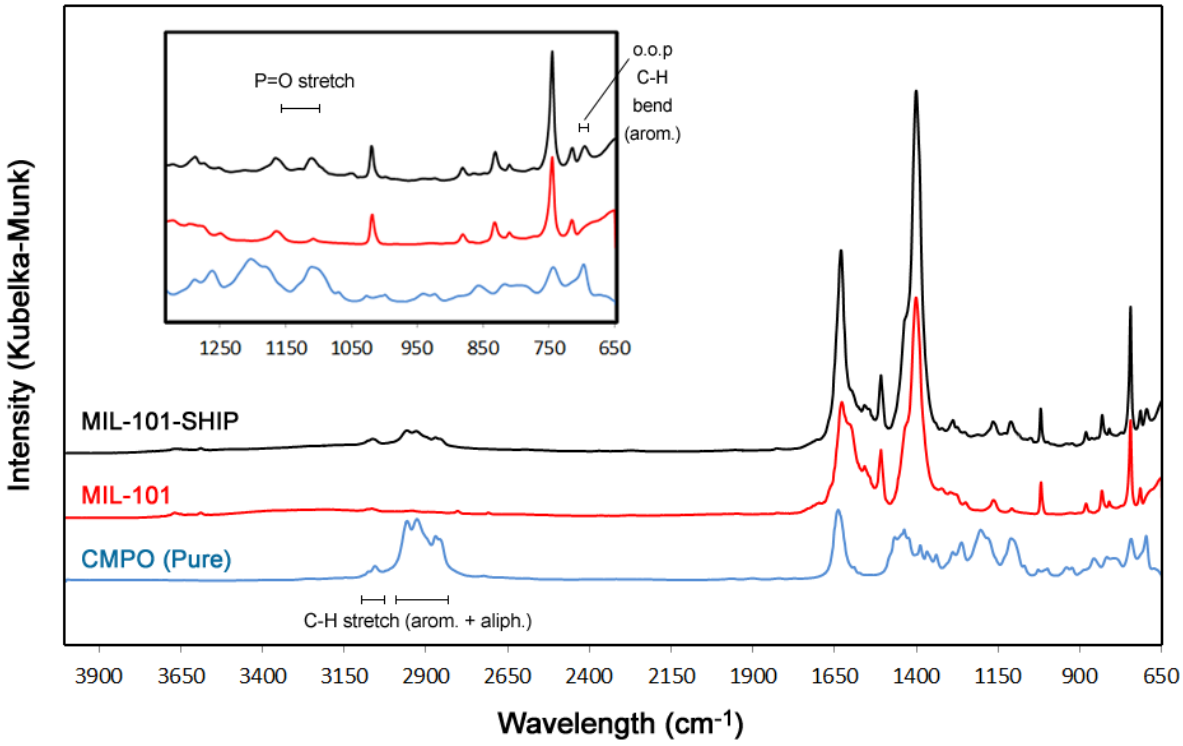

Fig. 2. DRIFTS spectra of the pristine MIL-101(Cr), the MIL-101-Ship and pure CMPO. (Inset: zoom on the 650 – 1300 cm^{-1} region).

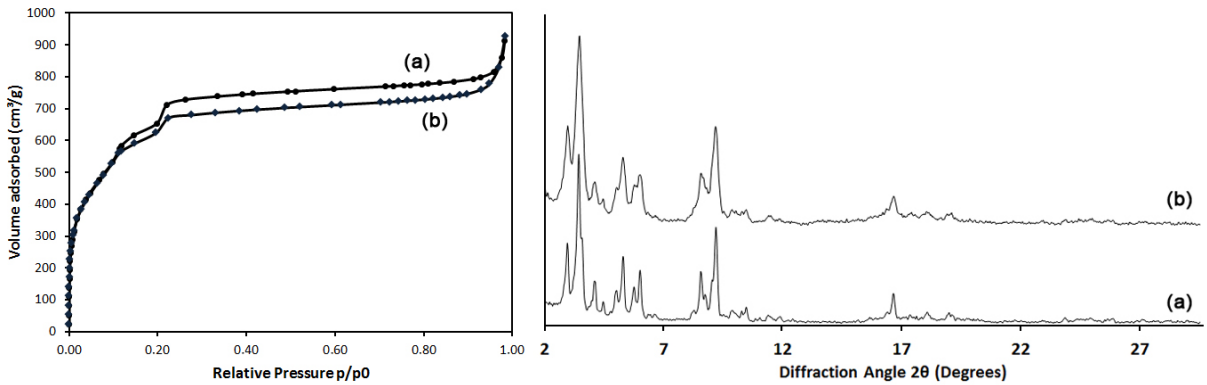

Fig. 3. Nitrogen adsorption isotherms (left) and X-ray diffraction patterns (right) of pristine MIL-101(Cr) (a) and MIL-101-Ship (b).

Table 1. Numerical N_2-adsorption data and loading calculations of MIL-101(Cr) and MIL-101-Ship.

	Specific Surface Area - Langmuir (m^2/g)	Specific Surface Area - BET (m^2/g)	Pore volume V_p (mL/g)	P content (wt. %)	CMPO loading (mmol/g)
MIL-101(Cr)	3400-3500	2500-2600	1.29	-	-
MIL-101-Ship	3200	2365	1.15	0.28 ± 0.03	0.09 ± 0.01*

*for reference: MIL-101 contains ~0.14mmol cages/g when pore volume = 1.3 mL/g

A small reduction in Langmuir surface area (as well as BET surface area and pore volume) is observed in the MIL-101-Ship, which can indicate the loading of the CMPO ligand inside the MOF. This reduction correlates well to the rather low CMPO loading. Via phosphorous XRF analysis, a loading of ~0.3 wt.% P was found, correlating to ~0.1 mmol CMPO/g. In addition to these powder analyses, the phosphorous-chromium ratio was calculated based on EDX data, demonstrating an average phosphorous loading of 0.12 mmol P/g, which is in good agreement with the initial XRF analysis. ADF-STEM and EDX imaging was applied to observe the MIL-101-Ship structure and P dispersion,

respectively. Highly crystalline particles with the typical MIL-101 truncated octahedron morphology and preferential {111} faceting are present. Phosphorous is found to be well dispersed throughout the material (Fig. 4).

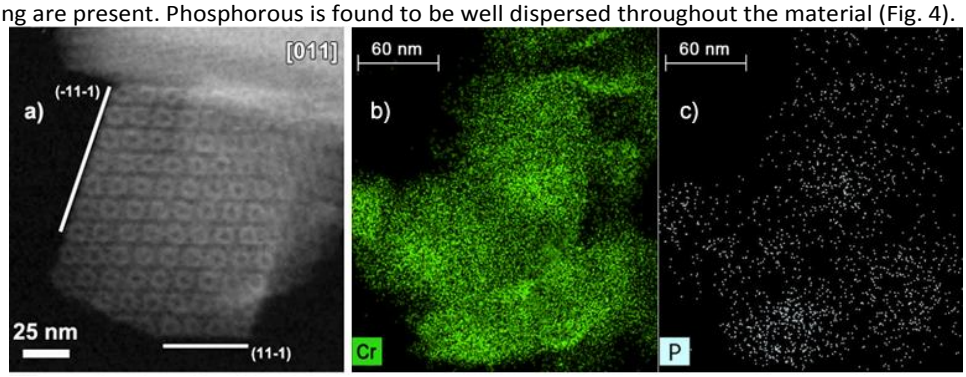

Fig. 4. (a)ADF-STEM image of a MIL-101 crystalline particle recorded along the [011] zone axis. (b,c) chromium (green) and phosphorous (white) EDX mapping, showing well dispersed P throughout the Cr-rich environment. Additional ADF-STEM images can be found in the Supporting information Fig. S.3.

3.3 Adsorbent Stability

An important requirement for adsorbents (and heterogeneous systems in general) is material stability. In the case of aqueous metal adsorption, a water-stable adsorbent is required, preferably with a high resistance to acidic conditions (adsorption/regeneration). In order to assess the MIL-101-Ship's resistance to these conditions, stability experiments were conducted in 1 M HCl and 1 M HNO_3. Based on XRD (Supporting information, Fig. S.4), the adsorbent shows a perfect resistance to both acidic conditions. This was already confirmed by Van Der Voort et al. for HCl[43]. Through XRF (phosphorous content analysis) it was found that no CMPO leached out during the acid treatments, which confirms that the CMPO is trapped within the cages of the MIL-101.

3.4 Adsorption Studies

Selectivity

Adsorption of U(VI) in the presence of various competing ions was performed with the MIL-101-Ship adsorbent and the pristine MIL-101, and evaluated in terms of the *Kd* values (Fig. 5). MIL-101-Ship shows a very high selectivity towards uranium, with nearly no uptake of the competing ions, which include both REEs (Eu, Gd, Nd, Y) and other cations (Al, Cd, Co, Cu, Mn, Ni, Pb, Zn). Fig. S.1 of the Supporting Information zooms in on the competing metals. It appears that the pristine MIL-101(Cr) possesses some affinity for U(VI) as well. We believe this is due to the presence of various hydroxylated uranium species ($[(UO_2)_x(OH)_y]^{2x-y}$), next to the dominant uranyl (UO_2^{2+}) species, at pH levels of ~ 4 and above. These hydroxylated species could weakly adsorb on the MIL-101 metal-oxide clusters. As the pH increases (> 4), more hydroxylated species are present instead of uranyl[59] and the interaction with MIL-101 increases, according to Bai *et al*.[45], who postulated that the multi-nuclear hydroxide complexes of U(VI) may be favored by the MIL-101.

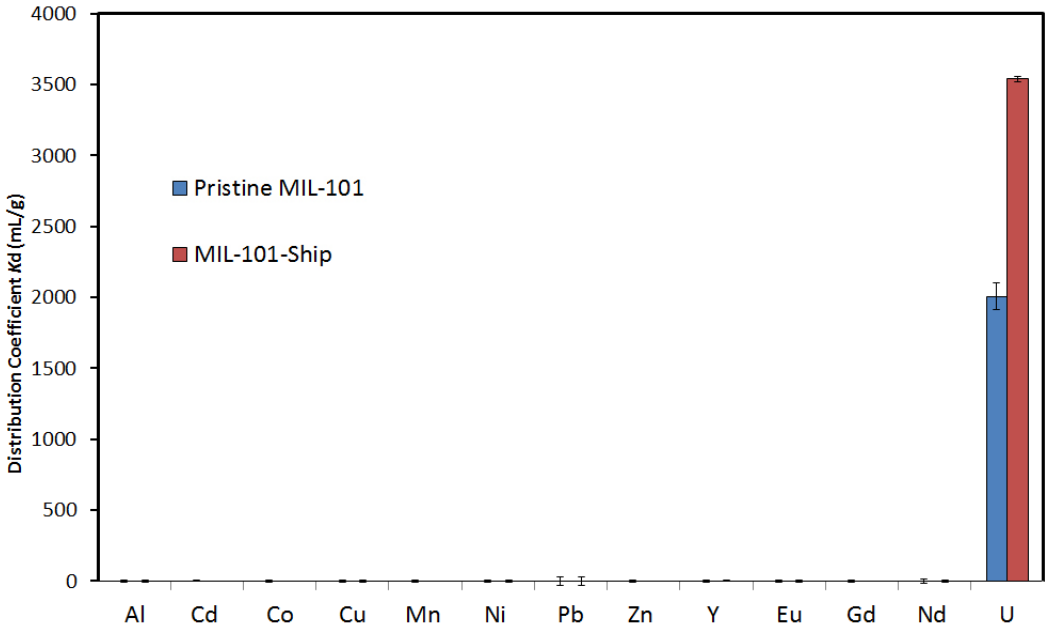

Fig. 5. Distribution coefficients (*Kd*) for the MIL-101-Ship (red) and pristine MIL-101 (blue), provided with standard deviations (error bars). C_0(M) = 1 mg/L each, pH: 4.0, L/S: 1000 mL/g, T = 25 °C, t = 24 hrs. A zoom on competing elements Kd can be found in the Supporting Information, Fig. S.1.

pH-dependency

The results are visualized in Fig. 6. At pH 6, both materials are active, with an increased uptake observed for MIL-101-Ship. At this pH level, hydroxylated uranium species are dominant, which might explain the affinity with the matrix (as mentioned above). At pH 3, U(VI) is entirely present as uranyl (UO_2^{2+}) and no interaction with the matrix should be expected. Indeed, only MIL-101-Ship adsorbs U(VI), whereas the pristine MIL-101 shows no uptake at all, which is a direct confirmation of the activity of CMPO within the cages of the MOF. At pH 0.5, none of the materials are active in the adsorption of U(VI). This result is interesting with respect to regeneration of the adsorbent, where a low pH could be used to effectively desorb the uranium.

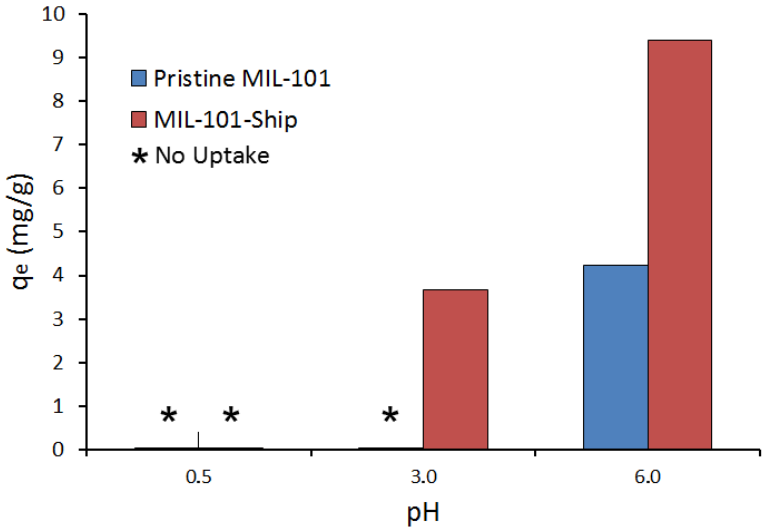

Fig. 6. U(VI) adsorption capacity in function of the pH for MIL-101-Ship (red) and the pristine MIL-101 (blue). C_0(U) = 30 mg/L, L/S: 1000 mL/g, T = 25 °C, t = 24 hrs.

Equilibrium study

A U(VI) equilibrium study on MIL-101-Ship was performed at two pH levels (3.0 and 4.0), as the uranium speciation at both pH levels might results in different adsorption characteristics. A continuous increase of U(VI) adsorption at both pH levels was observed with increasing initial uranium concentrations. The experimental data was fitted to the Langmuir and Freundlich models, both of which are frequently used to describe the adsorption mechanism of metals onto heterogeneous systems[60, 61]. Table 2 gives an overview of the obtained adsorption parameters for each model at the respective pH level. At pH 3, a good correlation is found with both models, however, regardless of the comparable correlation coefficient (R^2), the Langmuir model is deemed more suitable as it concerns metal adsorption through complexation with the CMPO ligand. This was also demonstrated by the pH-dependency study. The calculated maximum adsorption capacity via the Langmuir model is 5.32 mg U/g at pH 3. At pH 4, an increased U(VI) uptake was observed, which is again in line with the results for the pH dependency experiments. Both the Langmuir and Freundlich models have a similar high correlation, but selecting either of these is not straightforward, since at pH 4 a fraction of the uranium is present as UO_2OH^+ which can interact with the framework. Besides, adsorption of multinuclear uranyl hydroxide complexes would lead to a substantial increase in uranium uptake. Nonetheless, as most of the uranium at pH 4 is present as uranyl, the Langmuir model was used to estimate the maximum adsorption capacity at ~28 mg U/g. The Langmuir isotherms for both pH 3 and pH 4 are plotted in Fig. 7. Both the Langmuir and Freundlich isotherms can be found in the Supporting information, Fig. S.5.

Table 2. Adsorption parameters of U(VI) on MIL-101-Ship at pH 3 and pH 4, fitted to Langmuir and Freundlich models.

	Langmuir			Freundlich		
	q_{max} (mg/g)	K_L (L/mg)	R^2	n	K_F (mg/g (L/mg)$^{1/n}$)	R^2
pH 3	5.32	0.0215	0.9760	2.05	0.3833	0.9771
pH 4	27.99	0.0066	0.9833	1.43	0.4503	0.9894

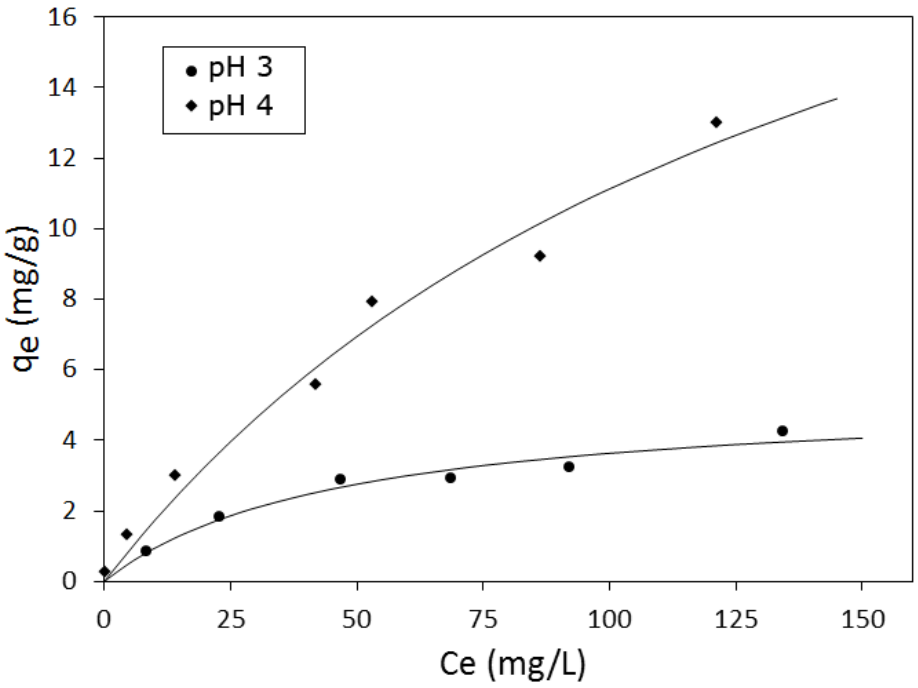

Fig. 7. U(VI) adsorption isotherm for MIL-101-Ship, fitted to the Langmuir model. pH: 3.0 and 4.0, L/S: 1000 mL/g, T = 25 °C, t = 24 hrs. Average value of duplicates.

Table 3 gives an overview of the MIL-101-Ship adsorption performance, compared to other reported MOF-based U(VI) adsorbents. On a pure capacity basis, our MIL-101-Ship does not surpass these reported adsorbents. This is mainly due to the limited amount of cages per gram in MIL-101 (0.14 mmol cages/g for a pore volume of 1.3 mL/g), which determines the amount of ligand which can be loaded into the structure. At ~0.09 mmol CMPO/g, we obtain a ~65 % theoretical filling ratio (assuming on average 1:1 ligand:cage). If each of these ligands were able to coordinate with one uranyl ion (which is generally the reported stoichiometry[44, 62]), the theoretical maximum uptake would be ~24 mg U(VI)/g (framework affinity and multinuclear complex coordination left aside). By normalizing the U(VI) adsorption to an active site basis (mg U(VI)/mmol active site), the MIL-101-Ship becomes competitive with the other reported adsorbents, and future work on improving the ligand loading could increase the uptake performance even further. Moreover, MIL-101-Ship excels at its zero-leaching behavior and high affinity for U(VI) with almost no competitive metal uptake.

Table 3. Overview of reported MOF-based U(VI) adsorbents and their adsorption performance, compared to MIL-101-Ship.

Adsorbent	**Saturation capacity (mg/g)**	**pH**	**Active sites (mmol/g)**	**Capacity/Active site (mg/mmol)**	**Ligand Leaching (1 run)**	**Selectivity for U(VI)**	**Reference**
MIL-101-Ship	5.32	3.0	0.09	59	0%	Highly over Al, Cd, Co, Cu, Mn, Ni, Pb, Zn, Y, Eu, Gd, Nd	This work
	27.99	4.0	0.09	310			
MIL-101-NH_2	90	5.5	1.63	55	0%	NM	[45]
MIL-101-ED*	200	5.5	1.28	156	30%*	Highly over Co, Ni, Zn, Sr, La, Nd, Sa, Yb	[45]
MIL-101-DETA*	350	5.5	0.72	486	30%*	Highly over Co, Ni, Zn, Sr, La, Nd, Sa, Yb	[45]
MOF-76	300	3.0	-	-	-	Highly over Sr, Cs, Cr, Co, Ni. Medium over Pb, Zn	[42]
UiO-68-$P(O)(OEt)_2$	217	2.5	ligand:linker 1:1	-	NM	NM	[44]
$Zn(H_3BTC)(L).(H_2O)_2$	115	2.0	NM**	-	-	NM	[63]
Zn-MOF-74 w/ Coumarin (11.7 wt%)	360	4.0	0.8	450	NM	NM	[46]

ED: ethylenediamine, DETA: diethylentriamine, H_3BTC: 1,3,5-benzenetricarboxylic acid, L: N4,N4'-di(pyridin-4-yl) biphenyl-4,4'-dicarboxamide), *: grafting via coordinatively unsaturated sites (CUS), **: ligands embedded in MOF structure, NM: not mentioned.

Kinetics

To evaluate the adsorption rate of U(VI) by the MIL-101-Ship, a series of identical adsorption tests were conducted with varying contact times (five minutes to 24 hours). The experiment was performed at pH 3.0, in order to obtain adsorption solely by the CMPO and avoid matrix interaction (see pH dependency). The experimental data was fitted to two kinetic models, namely the pseudo-first and pseudo-second-order model (Table 4). The best fit, namely pseudo-second-order, was plotted in Fig. 8. Both fits are also provided in the Supporting information, Fig. S.6. The pseudo-second order model indicates that the rate-limiting step is the surface adsorption that involves chemisorption, in which the removal of adsorbate from a solution is a result of physicochemical interactions between both phases[64]. The adsorption kinetics of U(VI) and other metal cations on ligand-functionalized adsorbents have often been described with pseudo-second-order kinetics[45, 65-67]. From this model, it can be calculated that after 375 minutes, over 95 % of the maximum U(VI) uptake is achieved and the adsorption gradually equilibrates. Within the first hour, 75 % uptake is achieved. In practical applications, a sorbent with fast kinetics but

smaller maximum uptake is often preferred over high uptakes and slow kinetics, and thus, the obtained kinetic profile is suitable for uses in adsorption column setups (dynamic conditions)[68].

Table 4. Parameters of the pseudo-first-order and pseudo-second-order kinetic models for adsorption of U(VI) on MIL-101-Ship. C_0: 30 mg/L, pH: 3.0, L/S: 1000 mL/g, T = 25 °C.

Pseudo-first-order model			Pseudo-second-order model		
q_e (mg/g)	k_1 (L/min)	R^2	q_e (calc) (mg/g)	k_2 (g/mg/min)	R^2
3.05	0.0308	0.935	3.23	0.016	0.975

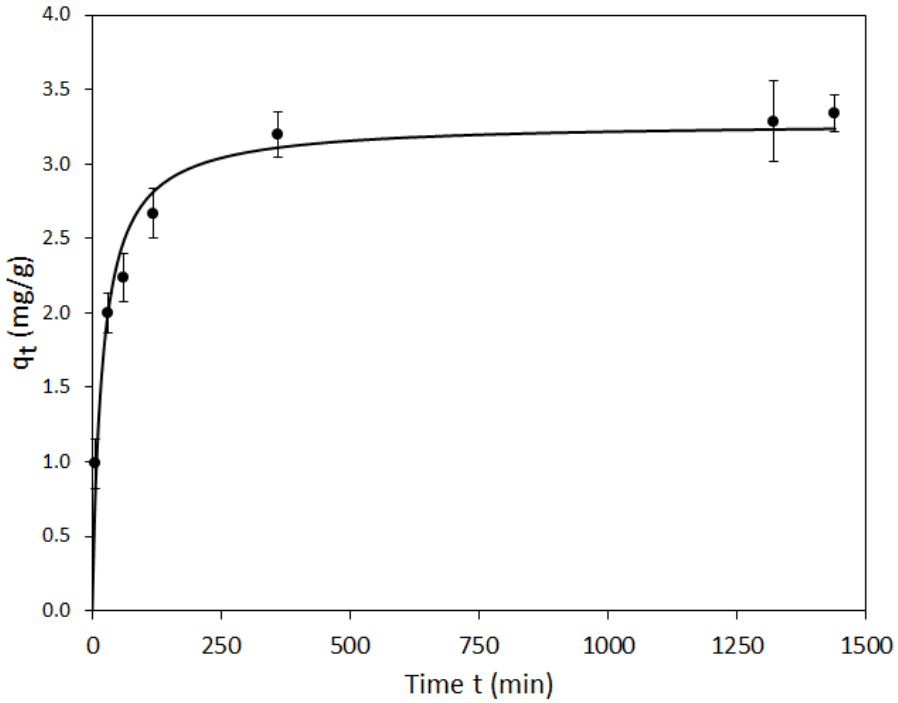

Fig. 8. Adsorption kinetics of U(VI) on MIL-101-Ship, fitted to the pseudo-second-order kinetic model. C_0(U) = 30 mg/L, L/S: 1000 mL/g, T = 25 °C, pH = 3. Average value of duplicates.

Regeneration and Reuse

Nitric acid (0.1 M) was used as regenerant, as a result of the pH dependency experiments. The results are plotted in Fig. 9. Stripping efficiencies of ~98% are obtained. A total of three complete cycles were performed. A constant uptake of about 10 mg U/g is observed, only slightly decreasing throughout the cycles. As three batch adsorption/desorption cycles comprise over 140 hours of turbulent contact with the acidic aqueous environment, additional XRD and XRF solid analyses were performed to investigate the adsorbent's resistance to this long-term exposure. The MIL-101 structure was found to remain perfectly intact, according to XRD, and the loss of CMPO was nearly negligible (<5%), confirming the remarkable stability of the adsorbent.

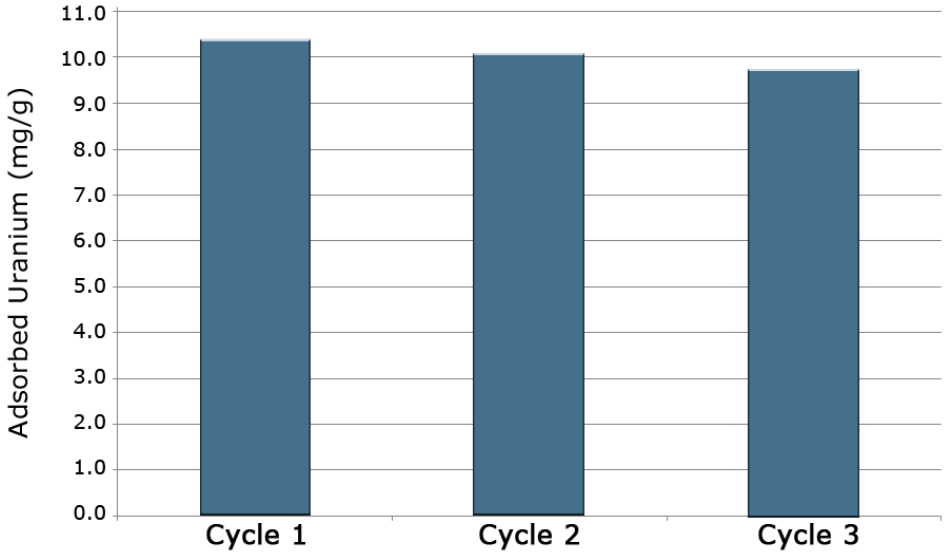

Fig. 9. Reusability results for MIL-101-Ship over three consecutive cycles, using 0.1 M HNO_3 as regenerant. L/S: 1000 mL/g, T = 25 °C, adsorption pH = 4.0.

4 Conclusion

We have reported the innovative combination of a highly water-stable MOF with selective chelating ligands, through a facile, cost-effective ship-in-a-bottle synthetic approach, yielding an effective adsorbent for uranium recovery from aqueous environments. The adsorbent consists of N,N-Diisobutyl-2-(octylphenylphosphoryl)acetamide (CMPO) trapped inside the cages of the MIL-101(Cr), making it an ideal compromise between homogeneous and heterogeneous systems. The synthesis comprises a one-step procedure and yields a leaching-free material with a loading of 0.09 mmol CMPO/g. The adsorption performance for U(VI) was investigated through an extensive adsorption study, including selectivity experiments, pH-dependency, equilibrium, kinetics, regeneration, and reuse. A very high selectivity was obtained for U(VI), with almost no uptake from competing metals, including rare earths and transition metals. The maximum adsorption capacity was calculated via the Langmuir model at 5.32 mg U/g (pH 3) and 27.99 mg U/g (pH 4). Kinetic experiments show that 75 % of the maximum uptake is achieved within the first hour of adsorption, after which the adsorption gradually equilibrates. Furthermore, the adsorbent can be effectively regenerated using 0.1 M HNO_3, and used for at least three cycles of uranium adsorption/desorption. It can therefore be concluded that the ship-in-a-bottle CMPO in MIL-101 system may be an efficient and feasible adsorbent for U(VI) recovery from aqueous environments, for instance as an effective uranium sequester in rare earth rich clay leachates or waste streams in phosphate rock processing. These streams are often neutralized to slightly acidic pH (4 - 5) in order to precipitate elements such as iron and thorium[15]. This is a suitable environment for our adsorbent to purify the obtained leachate from uranium. Besides, a selective adsorbent could be an ideal end-of-line technique to further increase the uranium recovery rate in industrial processes using solvent extractions.

Acknowledgements

The authors acknowledge the AUGent/UGent for financial support, Grant Number DEF12/AOP/008 fund IV1.

References

[1] International Energy Outlook 2016, in, U.S. Department of Energy, Washington, DC 20585, 2016.
[2] M. Salvatores, G. Palmiotti, Radioactive waste partitioning and transmutation within advanced fuel cycles: Achievements and challenges, Prog Part Nucl Phys, 66 (2011) 144-166.
[3] Uranium 2014: Resources, Production and Demand, in, OECD Nuclear Energy Agency and the International Atomic Energy Agency, 2014.
[4] J. Kim, C. Tsouris, R.T. Mayes, Y. Oyola, T. Saito, C.J. Janke, S. Dai, E. Schneider, D. Sachde, Recovery of Uranium from Seawater: A Review of Current Status and Future Research Needs, Separ Sci Technol, 48 (2013) 367-387.

[5] E.H.Y. AbowSlama, E. Ebraheem, A.K. Sam, Precipitation and purification of uranium from rock phosphate, J Radioanal Nucl Ch, 299 (2014) 815-818.
[6] F. Habashi, Correlation between the uranium content of marine phosphates and other rock constituents, Econ Geol, 57 (1962) 1081 - 1084.
[7] M.J. Lottering, L. Lorenzen, N.S. Phala, J.T. Smit, G.A.C. Schalkwyk, Mineralogy and uranium leaching response of low grade South African ores, Miner Eng, 21 (2008) 16-22.
[8] World Nuclear Association, Uranium from Phosphates, in, 2015.
[9] M. Walters, T. Baroody, W. Berry, Technologies for Uranium Recovery from Phosphoric Acid in: AIChE Central Florida Section, Florida, 2008.
[10] M.A. Maheswari, M.S. Subramanian, AXAD-16-3,4-dihydroxy benzoyl methyl phosphonic acid: a selective preconcentrator for U and Th from acidic waste streams and environmental samples, React Funct Polym, 62 (2005) 105-114.
[11] J. Veliscek-Carolan, Separation of actinides from spent nuclear fuel: A review, J Hazard Mater, 318 (2016) 266-281.
[12] M.C. Okeji, K.K. Agwu, F.U. Idigo, Assessment of Natural Radioactivity in Phosphate Ore, Phosphogypsum and Soil Samples Around a Phosphate Fertilizer Plant in Nigeria, B Environ Contam Tox, 89 (2012) 1078-1081.
[13] S. Bachmaf, B.J. Merkel, Sorption of uranium(VI) at the clay mineral-water interface, Environ Earth Sci, 63 (2011) 925-934.
[14] Y. Feng, H. Jiang, S. Li, J. Wang, X. Jing, Y. Wang, M. Chen, Metal-organic frameworks HKUST-1 for liquid-phase adsorption of uranium, Colloid Surface A, 431 (2013) 87-92.
[15] Z. Zhu, Y. Pranolo, C.Y. Cheng, Separation of uranium and thorium from rare earths for rare earth production - A review, Miner Eng, 77 (2015) 185-196.
[16] D. Mohan, C.U. Pittman, Activated carbons and low cost adsorbents for remediation of tri- and hexavalent chromium from water, J Hazard Mater, 137 (2006) 762-811.
[17] M. Imamoglu, O. Tekir, Removal of copper (II) and lead (II) ions from aqueous solutions by adsorption on activated carbon from a new precursor hazelnut husks, Desalination, 228 (2008) 108-113.
[18] X.Y. Guo, S.Z. Zhang, X.Q. Shan, Adsorption of metal ions on lignin, J Hazard Mater, 151 (2008) 134-142.
[19] D. Kolodynska, M. Geca, I.V. Pylypchuk, Z. Hubicki, Development of New Effective Sorbents Based on Nanomagnetite, Nanoscale Res Lett, 11 (2016) 1-10.
[20] G.P. Rao, C. Lu, F. Su, Sorption of divalent metal ions from aqueous solution by carbon nanotubes: A review, Sep Purif Technol, 58 (2007) 224-231.
[21] S.B. Wang, Y.L. Peng, Natural zeolites as effective adsorbents in water and wastewater treatment, Chem Eng J, 156 (2010) 11-24.
[22] K.G. Bhattacharyya, S. Sen Gupta, Adsorption of a few heavy metals on natural and modified kaolinite and montmorillonite: A review, Adv Colloid Interfac, 140 (2008) 114-131.
[23] J. Florek, S. Giret, E. Juere, D. Lariviere, F. Kleitz, Functionalization of mesoporous materials for lanthanide and actinide extraction, Dalton T, 45 (2016) 14832-14854.
[24] T.M. Budnyak, A.V. Strizhak, A. Gladysz-Plaska, D. Sternik, I.V. Komarov, D. Kolodynska, M. Majdan, V.A. Tertykh, Silica with immobilized phosphinic acid-derivative for uranium extraction, J Hazard Mater, 314 (2016) 326-340.
[25] M. Hua, S.J. Zhang, B.C. Pan, W.M. Zhang, L. Lv, Q.X. Zhang, Heavy metal removal from water/wastewater by nanosized metal oxides: A review, J Hazard Mater, 211 (2012) 317-331.
[26] M.R.L. Nascimento, O. Fatibello-Filho, L.A. Teixeira, Recovery of uranium from acid mine drainage waters by ion exchange, Miner Process Extr Metall Rev, 25 (2004) 129 - 142.
[27] A.C. Quieroz Ladeira, C.R. Goncalves, Influence of anionic species on uranium separation from acid mine water using strong base resins, J Hazard Mater, 148 (2007) 499-504.
[28] A. Mellah, S. Chegrouche, M. Barkat, The removal of uranium(VI) from aqueous solutions onto activated carbon: Kinetic and thermodynamic investigations, J Colloid Interf Sci, 296 (2006) 434-441.
[29] J. Canivet, A. Fateeva, Y.M. Guo, B. Coasne, D. Farrusseng, Water adsorption in MOFs: fundamentals and applications, Chem Soc Rev, 43 (2014) 5594-5617.
[30] J.R. Li, R.J. Kuppler, H.C. Zhou, Selective gas adsorption and separation in metal-organic frameworks, Chem Soc Rev, 38 (2009) 1477-1504.
[31] J.R. Li, Y.G. Ma, M.C. McCarthy, J. Sculley, J.M. Yu, H.K. Jeong, P.B. Balbuena, H.C. Zhou, Carbon dioxide capture-related gas adsorption and separation in metal-organic frameworks, Coordin Chem Rev, 255 (2011) 1791-1823.
[32] J. Liu, P.K. Thallapally, B.P. McGrail, D.R. Brown, J. Liu, Progress in adsorption-based CO2 capture by metal-organic frameworks, Chem Soc Rev, 41 (2012) 2308-2322.

[33] M.P. Suh, H.J. Park, T.K. Prasad, D.W. Lim, Hydrogen Storage in Metal-Organic Frameworks, Chem Rev, 112 (2012) 782-835.
[34] J. Lee, O.K. Farha, J. Roberts, K.A. Scheidt, S.T. Nguyen, J.T. Hupp, Metal-organic framework materials as catalysts, Chem Soc Rev, 38 (2009) 1450-1459.
[35] J.W. Liu, L.F. Chen, H. Cui, J.Y. Zhang, L. Zhang, C.Y. Su, Applications of metal-organic frameworks in heterogeneous supramolecular catalysis, Chem Soc Rev, 43 (2014) 6011-6061.
[36] B. Chen, S. Xiang, G. Qian, Metal-Organic Frameworks with Functional Pores for Recognition of Small Molecules, Accounts Chem Res, 43 (2010) 1115-1124.
[37] J.R. Li, J. Sculley, H.C. Zhou, Metal-Organic Frameworks for Separations, Chem Rev, 112 (2012) 869-932.
[38] R.C. Huxford, J. Della Rocca, W. Lin, Metal-organic frameworks as potential drug carriers, Curr Opin Chem Biol, 14 (2010) 262-268.
[39] P. Horcajada, R. Gref, T. Baati, P.K. Allan, G. Maurin, P. Couvreur, G. Ferey, R.E. Morris, C. Serre, Metal-Organic Frameworks in Biomedicine, Chem Rev, 112 (2012) 1232-1268.
[40] M. Kurmoo, Magnetic metal-organic frameworks, Chem Soc Rev, 38 (2009) 1353-1379.
[41] J. Rocha, L.D. Carlos, F.A. Almeida Paz, D. Ananias, Luminescent multifunctional lanthanides-based metal-organic frameworks, Chem Soc Rev, 40 (2011) 926-940.
[42] W. Yang, Z.Q. Bai, W.Q. Shi, L.Y. Yuan, T. Tian, Z.F. Chai, H. Wang, Z.M. Sun, MOF-76: from a luminescent probe to highly efficient U-VI sorption material, Chem Commun, 49 (2013) 10415-10417.
[43] K. Leus, T. Bogaerts, J. De Decker, H. Depauw, K. Hendrickx, H. Vrielinck, V. Van Speybroeck, P. Van Der Voort, Systematic study of the chemical and hydrothermal stability of selected "stable" Metal Organic Frameworks, Micropor Mesopor Mat, 226 (2016) 110-116.
[44] M. Carboni, C.W. Abney, S. Liu, W. Lin, Highly porous and stable metal-organic frameworks for uranium extraction, Chem Sci, 4 (2013) 2396-2402.
[45] Z.Q. Bai, L.Y. Yuan, L. Zhu, Z.R. Liu, S.Q. Chu, L.R. Zheng, J. Zhang, Z.F. Chai, W.Q. Shi, Introduction of amino groups into acid-resistant MOFs for enhanced U(VI) sorption, J Mater Chem A, 3 (2015) 525-534.
[46] L. Zhang, L.L. Wang, L.L. Gong, X.F. Feng, M.B. Luo, F. Luo, Coumarin-modified microporous-mesoporous Zn-MOF-74 showing ultra-high uptake capacity and photo-switched storage/release of U-VI ions, J Hazard Mater, 311 (2016) 30-36.
[47] F.W. Lewis, M.J. Hudson, L.M. Harwood, Development of Highly Selective Ligands for Separations of Actinides from Lanthanides in the Nuclear Fuel Cycle, Synlett, (2011) 2609-2632.
[48] Ion Exchange and Solvent Extraction: A Series of Advances, CRC Press, Florida, USA, 2009.
[49] D.M. Jiang, A.D. Burrows, K.J. Edler, Size-controlled synthesis of MIL-101(Cr) nanoparticles with enhanced selectivity for CO2 over N-2, Crystengcomm, 13 (2011) 6916-6919.
[50] T. Bogaerts, A. Van Yperen-De Deyne, Y.Y. Liu, F. Lynen, V. Van Speybroeck, P. Van Der Voort, Mn-salen@MIL101(Al): a heterogeneous, enantioselective catalyst synthesized using a 'bottle around the ship' approach, Chem Commun, 49 (2013) 8021-8023.
[51] R. Fazaeli, H. Aliyan, M. Moghadam, M. Masoudinia, Nano-rod catalysts: Building MOF bottles (MIL-101 family as heterogeneous single-site catalysts) around vanadium oxide ships, J Mol Catal a-Chem, 374 (2013) 46-52.
[52] J. Juan-Alcaniz, J. Gascon, F. Kapteijn, Metal-organic frameworks as scaffolds for the encapsulation of active species: state of the art and future perspectives, J Mater Chem, 22 (2012) 10102-10118.
[53] J. Juan-Alcaniz, E.V. Ramos-Fernandez, U. Lafont, J. Gascon, F. Kapteijn, Building MOF bottles around phosphotungstic acid ships: One-pot synthesis of bi-functional polyoxometalate-MIL-101 catalysts, J Catal, 269 (2010) 229-241.
[54] J.C. Jiang, O.M. Yaghi, Bronsted Acidity in Metal-Organic Frameworks, Chem Rev, 115 (2015) 6966-6997.
[55] M. Yoshizawa, J.K. Klosterman, M. Fujita, Functional Molecular Flasks: New Properties and Reactions within Discrete, Self-Assembled Hosts, Angew Chem Int Edit, 48 (2009) 3418-3438.
[56] M.H. Alkordi, Y.L. Liu, R.W. Larsen, J.F. Eubank, M. Eddaoudi, Zeolite-like metal-organic frameworks as platforms for applications: On metalloporphyrin-based catalysts, J Am Chem Soc, 130 (2008) 12639-12641.
[57] S. Bernt, V. Guillerm, C. Serre, N. Stock, Direct covalent post-synthetic chemical modification of Cr-MIL-101 using nitrating acid, Chem Commun, 47 (2011) 2838-2840.
[58] R.B. Ferreira, P.M. Scheetz, A.L.B. Formiga, Synthesis of amine-tagged metal-organic frameworks isostructural to MIL-101(Cr), Rsc Adv, 3 (2013) 10181-10184.
[59] Q.H. Fan, L.M. Hao, C.L. Wang, Z. Zheng, C.L. Liu, W.S. Wu, The adsorption behavior of U(VI) on granite, Environ Sci-Proc Imp, 16 (2014) 534-541.
[60] J. Febrianto, A.N. Kosasih, J. Sunarso, Y.H. Ju, N. Indraswati, S. Ismadji, Equilibrium and kinetic studies in adsorption of heavy metals using biosorbent: A summary of recent studies, J Hazard Mater, 162 (2009) 616-645.

[61] K. Folens, K. Leus, N.R. Nicomel, M. Meledina, S. Turner, G. Van Tendeloo, G. Du Laing, P. Van Der Voort, Fe3O4@MIL-101 – A Selective and Regenerable Adsorbent for the Removal of As Species from Water, Eur J Inorg Chem, 2016 (2016) 4395–4401
[62] A. Sengupta, M.S. Murali, S.K. Thulasidas, P.K. Mohapatra, Solvent system containing CMPO as the extractant in a diluent mixture containing n-dodecane and isodecanol for actinide partitioning runs, Hydrometallurgy, 147 (2014) 228-233.
[63] L.L. Wang, F. Luo, L.L. Dang, J.Q. Li, X.L. Wu, S.J. Liu, M.B. Luo, Ultrafast high-performance extraction of uranium from seawater without pretreatment using an acylamide- and carboxyl-functionalized metal-organic framework, J Mater Chem A, 3 (2015) 13724-13730.
[64] D. Robati, Pseudo-second-order kinetic equations for modeling adsorption systems for removal of lead ions using multi-walled carbon nanotube, Journal of Nanostructure in Chemistry, 3 (2013) 1-6.
[65] A.M. Donia, A.A. Atia, E.M.M. Moussa, A.M. El-Sherif, M.O. Abd El-Magied, Removal of uranium(VI) from aqueous solutions using glycidyl methacrylate chelating resins, Hydrometallurgy, 95 (2009) 183-189.
[66] Y.S. Ho, Review of second-order models for adsorption systems, J Hazard Mater, 136 (2006) 681-689.
[67] Y. Liu, L. Yuan, Y. Yuan, J. Lan, Z. Li, Y. Feng, Y. Zhao, Z. Chai, W. Shi, A high efficient sorption of U(VI) from aqueous solution using amino-functionalized SBA-15, J Radioanal Nucl Ch, 292 (2012) 803-810.
[68] L.S. Djokic, R. Pantovic, N. Stavretovic, R. Igic, Origin of Arsenic in Drinking Waters in the West Backa District of Serbia, in: M. Václavíková, K. Vitale, G.P. Gallios, L. Ivaničová (Eds.) Water Treatment Technologies for the Removal of High-Toxity Pollutants, Springer Science, 2010, pp. 41-50.